haematologica
Journal of the Ferrata Storti Foundation

High-cholesterol diet fuels myeloma progression, dysregulates adipokine expression *in vivo*, and impairs treatment response *ex vivo*

by Beatriz Gámez, Danielle J. Whipp, Srinivasa R. Rao, Emma V. Morris, Young Eun Park, Zeynep Kaya and Claire M. Edwards

Received: June 16, 2025.
Accepted: February 2, 2026.

Citation: Beatriz Gámez, Danielle J. Whipp, Srinivasa R. Rao, Emma V. Morris, Young Eun Park, Zeynep Kaya and Claire M. Edwards. High-cholesterol diet fuels myeloma progression, dysregulates adipokine expression in vivo, and impairs treatment response ex vivo.
Haematologica. 2026 Feb 12. doi: 10.3324/haematol.2025.288286 [Epub ahead of print]

High-cholesterol diet fuels myeloma progression, dysregulates adipokine expression *in vivo*, and impairs treatment response *ex vivo*

Beatriz Gámez[1,2], Danielle J. Whipp[1], Srinivasa R. Rao[1,2], Emma V. Morris[1], Young Eun Park[1,2], Zeynep Kaya[1] and Claire M. Edwards[1, 2,3].

[1] Nuffield Department of Surgical Sciences, University of Oxford, Oxford, UK.

[2]Oxford Translational Myeloma Centre, University of Oxford, Oxford, UK

[3] Nuffield Department of Orthopaedics, Rheumatology and Musculoskeletal Sciences, University of Oxford, Oxford, UK.

Running title: High cholesterol fuels myeloma progression

*** Corresponding author:** Claire M. Edwards. Nuffield Department of Orthopaedics, Rheumatology and Musculoskeletal Sciences, University of Oxford, Oxford, UK. Botnar Research Centre. Old Rd, Oxford OX3 7LD.

Tel.: +44 (0) 1865 227307; Email: claire.edwards@ndorms.ox.ac.uk

Authors' contributions: B.G and C.M.E conceived the experiments. B.G planned the experiments. B.G and D.J.W performed the experiments. B.G analysed the data. S.R contributed to sample preparation and analysed RNA-seq data. Z.K , E.V.M and Y.P contributed to in vivo work and sample preparation. B.G and C.M.E wrote the manuscript.

Authors' disclosures: The authors declare no potential conflicts of interest.

Data sharing: RNA sequencing data from this article is available from the authors upon request.

Funding: This research was funded by Blood Cancer UK, Rosetrees, Cancer Research UK, the National Institute for Health Research (NIHR) Oxford Biomedical Research Centre (BRC) and funds from the CRRMF and Equality and Diversity Unit (University of Oxford). The views

expressed are those of the author(s) and not necessarily those of the NHS, the NIHR or the Department of Health.

Acknowledgements: We are grateful to the Multiple Myeloma Research Foundation Personalized Medicine Initiatives (https://research.themmrf.org and www.themmrf.org).

Multiple myeloma (MM) is an incurable hematologic cancer where malignant plasma cells accumulate in the bone marrow (BM) [1]. MM evolves from the premalignant disorder monoclonal gammopathy of undetermined significance (MGUS) and despite recent advances in therapy, MM remains incurable largely due to drug resistance [2]. Obesity is the second leading cause of cancer and has been linked to several types of malignancies, including MM [3, 4]. Although the exact mechanism by which obesity impacts MM pathogenesis is still unclear, it is the only modifiable risk known for MM and so it provides hope for dietary and lifestyle interventions.

Strongly associated with obesity is high cholesterol. Several studies have shown that MM patients have a reduction in total cholesterol, LDL and high-density lipoproteins (HDL) in plasma compared to healthy individuals with more evident changes in later stages of disease [5, 6]. However, despite significant efforts to elucidate the role of total cholesterol or LDL in cancer, little is known about the effect of high circulating cholesterol and LDL levels in MM disease.

To understand the effect of cholesterol on myeloma progression in vivo, C57BL/KaLwRij mice were placed on a 2% cholesterol diet for four weeks after which time mice showed increased circulating LDL (Fig 1A & Fig S1A) with no changes in body weight (Fig S1B).

Increased liver weight (Fig S1C & Fig S1D) and signs of fatty liver disease were seen (data not shown). Mice were then inoculated intravenously with 5TGM1-GFP cells and cholesterol diet was either halted at this point or maintained continuously (Fig S1A). LDL levels remained elevated only in the animals fed continuously with the cholesterol diet (Fig 1B), which also showed a significant increase in tumour burden and serum paraprotein (IgG2b) levels compared to the myeloma control

group (Fig 1C-D). No significant changes in spleen tumour burden or weight were detected in any of the cholesterol diet groups suggesting a bone-specific effect of LDL (Fig 1E & Fig S1E). Myeloma cells from continuously cholesterol-fed animals had a higher proportion of highly lipidtox+ve cells demonstrating a higher intracellular lipid content (Fig 1F-G). Initiation of the cholesterol-enriched diet at the time of tumour inoculation (Fig S1A), resulted in significantly higher BM tumour burden and bone lesions with no changes in spleen (Fig1H-J). All animal procedures were conducted in accordance with the Animals Scientific Procedures Act of 1986 (UK) and approved by the University of Oxford Animal Welfare and Ethical Review Body (Home Office Project Licenses PCCCC8952 and PP9500304).

Myeloma is heavily dependent on the BM microenvironment, therefore we investigated the impact of dietary cholesterol on local, as compared to systemic, factors. VLDL/LDL cholesterol fraction in BM plasma was increased in cholesterol-fed mice (Fig 2A). Using an adipokine proteome profiler we detected elevated levels of the adipokine resistin after cholesterol diet and in myeloma-bearing mice specifically in BM plasma (Fig 2B-C). We corroborated the increase in resistin by ELISA, demonstrating a significant increase following cholesterol diet in BM plasma (Fig 2D) but not blood (Fig 2E). Interestingly, relative to all adipokines, resistin was one of the highest expressed adipokines in blood, but was reduced in BM plasma highlighting the differences in the local and systemic soluble milieu (Fig 2SA-B). Tumour-bearing mice showed significantly higher resistin in BM plasma (Fig 2F), with a positive correlation between BM plasma resistin and IgG2bκ in myeloma-bearing mice that was lost with cholesterol treatment (Fig 2G).

To further investigate the role of LDL in myeloma, we studied the effect of LDL on myeloma growth and drug resistance, focusing on the proteasome inhibitor

bortezomib, following recent evidence for the sensitivity of bortezomib-resistant myeloma cells to a cholesterol-lowering drug (10). LDL reversed the reduction in myeloma cell viability caused by delipidation or metabolic stress (no FBS) (Fig.S2C). Very-low-density lipoprotein (VLDL) had no effect on viability of JJN3 or MM1S whereas in 5TGM1-GFP cells, VLDL had similar effects to LDL suggesting differential sensitivities of myeloma cells to lipid depletion and cholesterol levels (Fig S2C). In support of this, lipid depletion and metabolic stress increased LDL uptake, with variability in uptake between cell lines (Fig S2D-G). LDL was incorporated after 3h (Fig 3A) and completely blocked the effect of the proteasome inhibitor bortezomib to reduce viability in metabolically-stressed myeloma cells (Fig S3A-B). LDL-treated bone marrow isolated from myeloma-bearing mice was used ex vivo, showing the same level of protection from bortezomib (Fig 3B).

Bortezomib reduced viability and induced expression of apoptotic markers that was reversed upon addition of LDL prior to bortezomib treatment (Fig 3C). In cell cycle analysis, LDL also reduced the apoptotic fraction that was increased following bortezomib treatment (Fig S3C). Carfilzomib, MG132, metformin or dexamethasone were also tested, however LDL had no effect on drug response (Fig S2D-G). To further investigate how LDL induces bortezomib resistance, we studied proteasome activity and performed cycloheximide chase assays. LDL pre-treated JJN3 myeloma cells had no change in proteasome activity after bortezomib treatment (Fig 3D, Fig S3H-I).

Fluctuations in cholesterol accumulation can induce changes in plasma membrane fluidity and composition and can alter molecular pathways associated with drug uptake, efflux and chemoresistance, including caveolin-1 [7-9]. Bortezomib induced a dose-dependent decrease in membrane fluidity in JJN3 myeloma cells. LDL-

pretreated cells also exhibited a reduction in membrane fluidity but with no further changes following bortezomib treatment (Fig S3J). LDL increased caveolin-1 expression in myeloma cells (Fig S4A) and prevented the reduction in caveolin-1 and MDR1 expression induced by bortezomib (Fig S4B). In support of this, bortezomib-resistant MM cells were found to have an increase in caveolin-1 and MDR1, alongside a decrease in INSIG1 which regulates cholesterol metabolism (Fig S4C).

RNA-sequencing (RNA-Seq) was performed on JJN-3 myeloma cells in the presence and absence of LDL and bortezomib. Differential expression gene (DEG) analysis revealed changes in expression of genes key to cholesterol synthesis (e.g. HMGCS1 or INSIG1) after bortezomib treatment, with LDL pre-treatment restoring the transcriptomic profile of bortezomib-treated cells to that of control (Fig 3E, Fig S4D). Accordingly, PCA plot demonstrated a clear distinction of the bortezomib treated group, and LDL pretreated samples grouped together with the untreated (Fig S4E). When GSEA hallmark gene sets were analysed, the hallmark apoptosis gene set was enriched in bortezomib-treated cells compared to LDL-bortezomib treated (Fig S4F). Gene set expression analysis (GSEA) revealed a significant effect of bortezomib on reactome cholesterol biosynthesis and cholesterol homeostasis (Fig S4G). Further analysis using the ShinyGO tool and top 1000 down-regulated genes demonstrated proteasome pathway enrichment in bortezomib samples as compared to LDL-bortezomib treated (Fig S5A). Interestingly, ferroptosis was also among the most enriched pathways, demonstrated by both ShinyGO and GSEA (Fig S5A-B). Only a small number of differentially expressed genes were found after LDL treatment compared to untreated (Fig S5C-D). ShinyGO analysis of all DEG revealed ferroptosis as one of only 2 modulated pathways (Fig S5E) and GSEA

using the WP Ferroptosis gene set revealed a significant effect of LDL on ferroptosis in both control and bortezomib-treated cells (Fig S5A).

Using data from the CoMMpass-MMRF database, a list of 7 mevalonate pathway-related genes (M46454 human gene set, GSEA) was used to study whether their expression had an impact on probability of first response in patients. Expression of HMGCR and HMGCS1, key genes in the mevalonate pathway, had an effect in patients that were placed on bortezomib-based therapies as first option but not for other therapies, however differences were not significant after p-value correction (data not shown). Further analysis studying the combined effect of both genes showed that they were determinant for the response to therapy only in patients under bortezomib therapy, demonstrating the importance of cholesterol metabolism in the response to bortezomib (Fig 3F-G).

In this study, high dietary cholesterol increased myeloma tumour burden in the BM, accompanied by increased lipid content in myeloma cells. Mice were fed standard chow diet supplemented with 2% cholesterol. Unlike a Western diet, which combines high fat, high sucrose, and added cholesterol to model obesity and metabolic syndrome, this approach isolates the specific contribution of cholesterol without the confounding effects of excess fat or sugar. Proteomic profiling revealed elevated resistin, an adipokine associated with both hypercholesterolemia and myeloma, positively correlating with IgG2b levels. Resistin therefore emerges as a potential biomarker and mediator of tumour–bone crosstalk.

Mechanistically, LDL-cholesterol induced resistance to the proteasome inhibitor bortezomib. Myeloma cells efficiently internalised LDL, which fully abrogated bortezomib-induced apoptosis and reversed its transcriptional signature, particularly

under metabolic stress. This effect was specific to bortezomib. RNA-seq and enrichment analyses implicated ferroptosis in mediating drug resistance, consistent with evidence linking cholesterol to ferroptosis evasion and the ability of cholesterol-lowering agents to effectively inhibiting bortezomib-resistant myeloma cells [10].

Our in vitro data demonstrates that LDL pre-treatment of myeloma cells altered membrane fluidity and increased caveolin-1 expression, a protein linked to redox homeostasis, adhesion and bortezomib resistance [11]. Modulation of membrane fluidity may influence not only intracellular trafficking and therapeutic response but also the diapedesis of myeloma cells, potentially modulating myeloma cell homing to the bone marrow. In silico patient analysis using the MMRF CoMMpass study data supported these findings: the level of expression of key genes in the mevalonate pathway (HMGCS1, HMGCR) predicted outcomes only in patients with bortezomib-based therapy as a first option.

Resistin was elevated in the BM niche following high cholesterol, consistent with the cholesterol-oriented metabolism of BM adipocytes [12]. Known to induce multidrug tolerance through ABC transporter upregulation, resistin may contribute to bortezomib resistance [13-15].

In summary, our findings reveal the impact of high cholesterol on myeloma progression and bortezomib resistance and provide insight into the cellular mechanisms that underly this, identifying resistin as a potential mediator within the tumour-bone microenvironment. Furthermore, our studies provide important mechanistic insight to facilitate optimal pharmacological or dietary intervention strategies.

REFERENCES

1. Kumar SK, Rajkumar V, Kyle RA, et al. Multiple myeloma. Nat Rev Dis Primers. 2017;3:17046.

2. Malard F, Neri P, Bahlis NJ, et al. Multiple myeloma. Nat Rev Dis Primers. 2024;10(1):45.

3. Morris EV, Edwards CM. Bone Marrow Adipose Tissue: A New Player in Cancer Metastasis to Bone. Front Endocrinol (Lausanne). 2016;7:90.

4. Morris EV, Edwards CM. Adipokines, adiposity, and bone marrow adipocytes: Dangerous accomplices in multiple myeloma. J Cell Physiol. 2018;233(12):9159-9166.

5. Yavasoglu I, Tombuloglu M, Kadikoylu G, Donmez A, Cagirgan S, Bolaman Z. Cholesterol levels in patients with multiple myeloma. Ann Hematol. 2008;87(3):223-228.

6. Hungria VT, Latrilha MC, Rodrigues DG, Bydlowski SP, Chiattone CS, Maranhao RC. Metabolism of a cholesterol-rich microemulsion (LDE) in patients with multiple myeloma and a preliminary clinical study of LDE as a drug vehicle for the treatment of the disease. Cancer Chemother Pharmacol. 2004;53(1):51-60.

7. Kozalak G, Butun I, Toyran E, Kosar A. Review on Bortezomib Resistance in Multiple Myeloma and Potential Role of Emerging Technologies. Pharmaceuticals (Basel). 2023;16(1):111.

8. Chan NN, Yamazaki M, Maruyama S, et al. Cholesterol Is a Regulator of CAV1 Localization and Cell Migration in Oral Squamous Cell Carcinoma. Int J Mol Sci. 2023;24(7):6035.

9. Zhao X, Lian X, Xie J, Liu G. Accumulated cholesterol protects tumours from elevated lipid peroxidation in the microenvironment. Redox Biol. 2023;62:102678.

10. Zhang H, Wang H, Hu Y, et al. Targeting PARP14 with lomitapide suppresses drug resistance through the activation of DRP1-induced mitophagy in multiple myeloma. Cancer Lett. 2024;588:216802.

11. Zhan D, Du Z, Zhang S, et al. Targeting Caveolin-1 in Multiple Myeloma Cells Enhances Chemotherapy and Natural Killer Cell-Mediated Immunotherapy. Adv Sci (Weinh). 2024;12(4):e2408373.

12. Attane C, Esteve D, Chaoui K, et al. Human Bone Marrow Is Comprised of Adipocytes with Specific Lipid Metabolism. Cell Rep. 2020;30(4):949-958.e946.

13. Kim HJ, Lee YS, Won EH, et al. Expression of resistin in the prostate and its stimulatory effect on prostate cancer cell proliferation. BJU Int. 2011;108(2 Pt 2):E77-83.

14. Kuo CH, Chen KF, Chou SH, et al. Lung tumor-associated dendritic cell-derived resistin promoted cancer progression by increasing Wolf-Hirschhorn syndrome candidate 1/Twist pathway. Carcinogenesis. 2013;34(11):2600-2609.

15. Pang J, Shi Q, Liu Z, et al. Resistin induces multidrug resistance in myeloma by inhibiting cell death and upregulating ABC transporter expression. Haematologica. 2017;102(7):1273-1280.

Figure 1. A high cholesterol diet increases LDL and bone marrow tumour burden in vivo in C57BL/6 KaLwRij mice.

(**A**) C57BL/6 KaLwRij mice were fed with either control or high cholesterol diet for 4 weeks and serum LDL was measured. Mice were then randomly distributed into either control or tumour-bearing mice (myeloma) and inoculated with $1.5x10^6$ 5TGM1-GFP cells. Cholesterol non-tumour mice and cholesterol pre-treatment myeloma mice had cholesterol diet halted at time of inoculation. (**B**) LDL in serum was measured at endpoint. (**C**) Proportion of 5TGM1 GFP +ve tumour cells in bone marrow. (**D**) IgG2bκ levels in serum. (**E**) Proportion of GFP+ve myeloma cells in spleen. (**F**) Lipid content of GFP+ve myeloma cells from bone marrow quantified by lipidtox stain and flow cytometry. **(G)** Representative image acquired by confocal microscopy showing incorporation of far-red lipidtox in JJN3. In separate experiments, cholesterol diet was given from time of inoculation and GFP+ve myeloma cells in bone marrow (**H**) and spleen tumour burden (**I**) were quantitated by flow cytometry. (**J**) Number of bone lesions counted from microCT images. For 2 group comparison, two-tailed Student's t-test was performed. *p< 0.05, **p < 0.01 and ***p < 0.001. For more than 2 groups one-way anova analysis was performed. For C, **p < 0.01 and ***p < 0.001 compared to animals on control and cholesterol diets with no-tumour. ##p < 0.01 compared to myeloma cholesterol pre-treatment and ^{a}p < 0.05 compared to myeloma on control diet. For E, *p< 0.05 and ***p < 0.001 compared to control with no-tumour in control diet or cholesterol diet. If not otherwise indicated, *p< 0.05, **p < 0.01 and ***p < 0.001 compared to control with no-tumour. Results are presented as mean ± SEM.

Figure 2. Adipokine profiles identify increased resistin in bone marrow in response to high cholesterol or myeloma.

(**A**) LDL/VLDL-C ratio in the bone marrow of C57BL/6 KaLwRij mice after 4 weeks of high cholesterol diet. Heat maps show relative expression of adipokines in blood (**B**) and bone marrow plasma (**C**) of a non-tumour mouse on cholesterol diet (CHOL), myeloma-bearing mouse (MM) and myeloma-bearing mouse on cholesterol diet (MM CHOL) compared to non-tumour control. Cholesterol diet was given continuously in all groups. (**D**) Relative resistin expression (expressed as fold-increase compared to control) in bone marrow plasma from non-tumour mice fed with control diet (CTR), cholesterol diet for 4 weeks (CHOL 4w) or cholesterol diet for 8 weeks (CHOL 8w). (**E**) Resistin expression in blood from control or cholesterol fed animals for 8 weeks. (**F**) Relative resistin expression (expressed as fold-increase compared to control) in bone marrow plasma in control non-tumour mice (CTR), myeloma-bearing mice (MM) and myeloma-bearing mice on cholesterol diet (MM CHOL) from inoculation. (**G**) Pearson correlation of IgG2bκ paraprotein and resistin levels in non-tumour mice in control diet (8 pairs of XY), tumour-bearing mice (13 pairs of XY) and tumour-bearing mice on cholesterol diet (12 pairs of XY). For 2 group comparison, two-tailed Student's t-test was performed. For more than 2 groups one-way anova analysis was performed. If not otherwise indicated, *$p < 0.05$ and ***$p < 0.001$ compared to control. Results are presented as mean ± SEM.

Figure 3. LDL induces resistance to bortezomib and changes in the cholesterol pathway.

(A) 5TGM1-GFP were cultured in serum-free conditions and treated with pHrodo^{TM} red-LDL for 3 hours. 40x magnification. (**B**) Whole BM was isolated from myeloma-bearing mice, seeded with no FBS media and treated with 30 µg/ml LDL for 3 hours before 24 hour bortezomib treatment. Viability was quantitated by alamar blue (n = 3). Tumour cell viability was assessed by flow cytometry as GFP+ve cells compared to control. (**C**) JJN3 were cultured in serum-free conditions ± LDL for 3 hours before bortezomib treatment for 24 hours. Apoptotic markers cPARP and short Mcl-1 were measured by western blotting with concurrent viability quantitation. (**D**) JJN3 myeloma cells were treated in the presence and absence of LDL and bortezomib and proteasome activity measured using a proteasome 20S activity assay kit. (**E**) JJN3 myeloma cells were treated in the presence and absence of LDL and bortezomib and RNA-Seq performed. Heatmap showing differential expression gene (DEG) analysis from bortezomib vs. control cells. CoMMpass study data analysis showing the impact of HMGCR and HMGCS1 expression on the probability of first response over time in patients with bortezomib-based therapies as first option (**F**) and patients with other therapies (**G**). One-way ANOVA analysis was performed. For B ***$p < 0.001$ compared to control non-LDL condition. For B ***$p < 0.001$ compared to control non-bortezomib treated condition, ###$p < 0.001$ compared to bortezomib treated no-LDL condition. For D, *$p< 0.05$, **$p < 0.01$ compared to control (no bortezomib, no LDL). Results are presented as mean ± SEM.

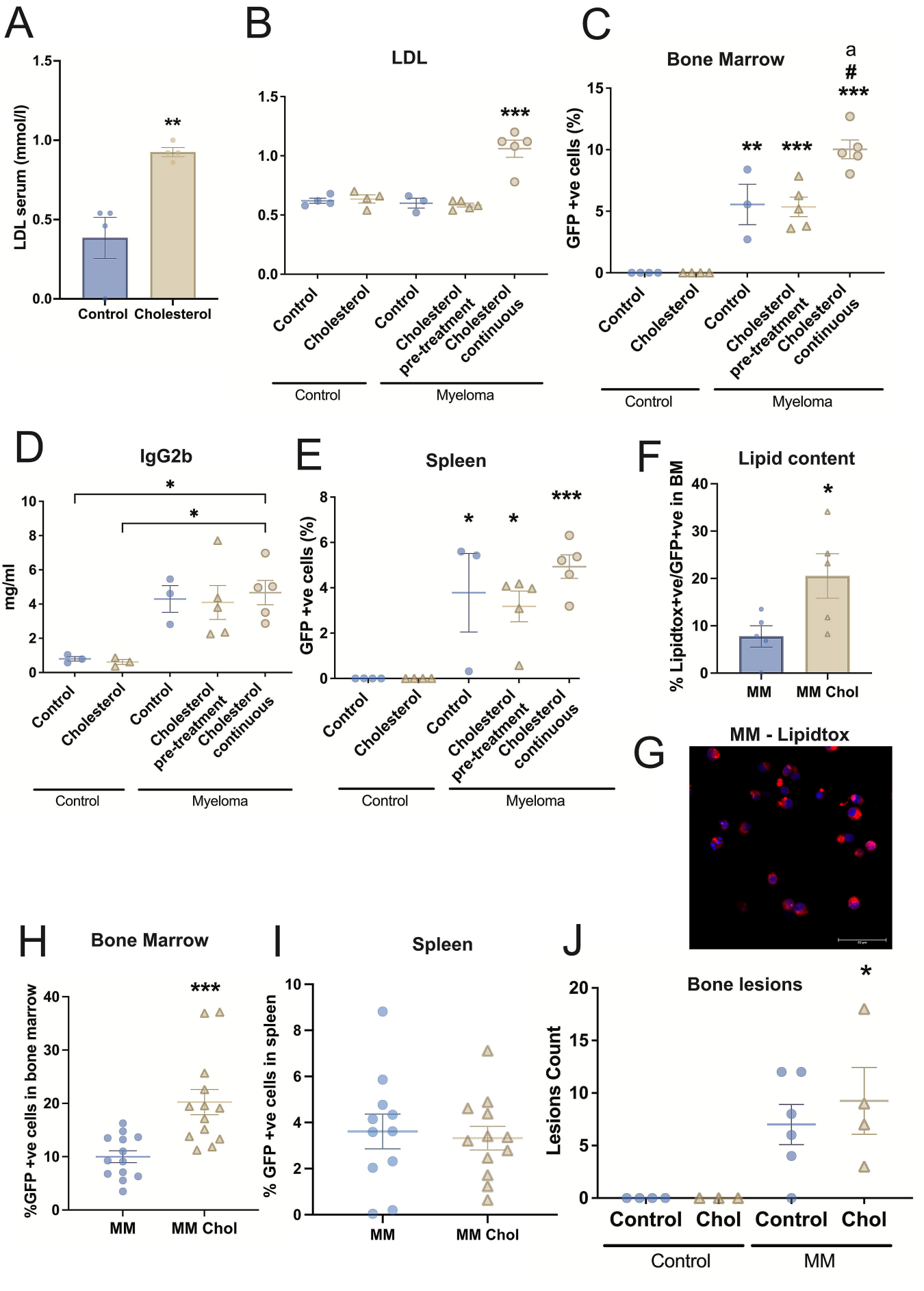
A
LDL serum (mmol/l)
1.5
1.0
0.5
0.0
**
Control
Cholesterol
B
LDL
1.5
1.0
0.5
0.0
***
Control
Cholesterol
Control
Cholesterol pre-treatment
Cholesterol continuous
Control
Myeloma
C
Bone Marrow
a
#
***
GFP +ve cells (%)
15
10
5
0
**
***
Control
Cholesterol
Control
Cholesterol pre-treatment
Cholesterol continuous
Control
Myeloma
D
IgG2b
mg/ml
10
8
6
4
2
0
*
*
Control
Cholesterol
Control
Cholesterol pre-treatment
Cholesterol continuous
Control
Myeloma
E
Spleen
GFP +ve cells (%)
8
6
4
2
0
*
*
***
Control
Cholesterol
Control
Cholesterol pre-treatment
Cholesterol continuous
Control
Myeloma
F
Lipid content
% Lipidtox+ve/GFP+ve in BM
40
30
20
10
0
*
MM
MM Chol
G
MM - Lipidtox
H
Bone Marrow
%GFP +ve cells in bone marrow
40
30
20
10
0
***
MM
MM Chol
I
Spleen
% GFP +ve cells in spleen
10
8
6
4
2
0
MM
MM Chol
J
Bone lesions
Lesions Count
20
15
10
5
0
*
Control
Chol
Control
Chol
Control
MM

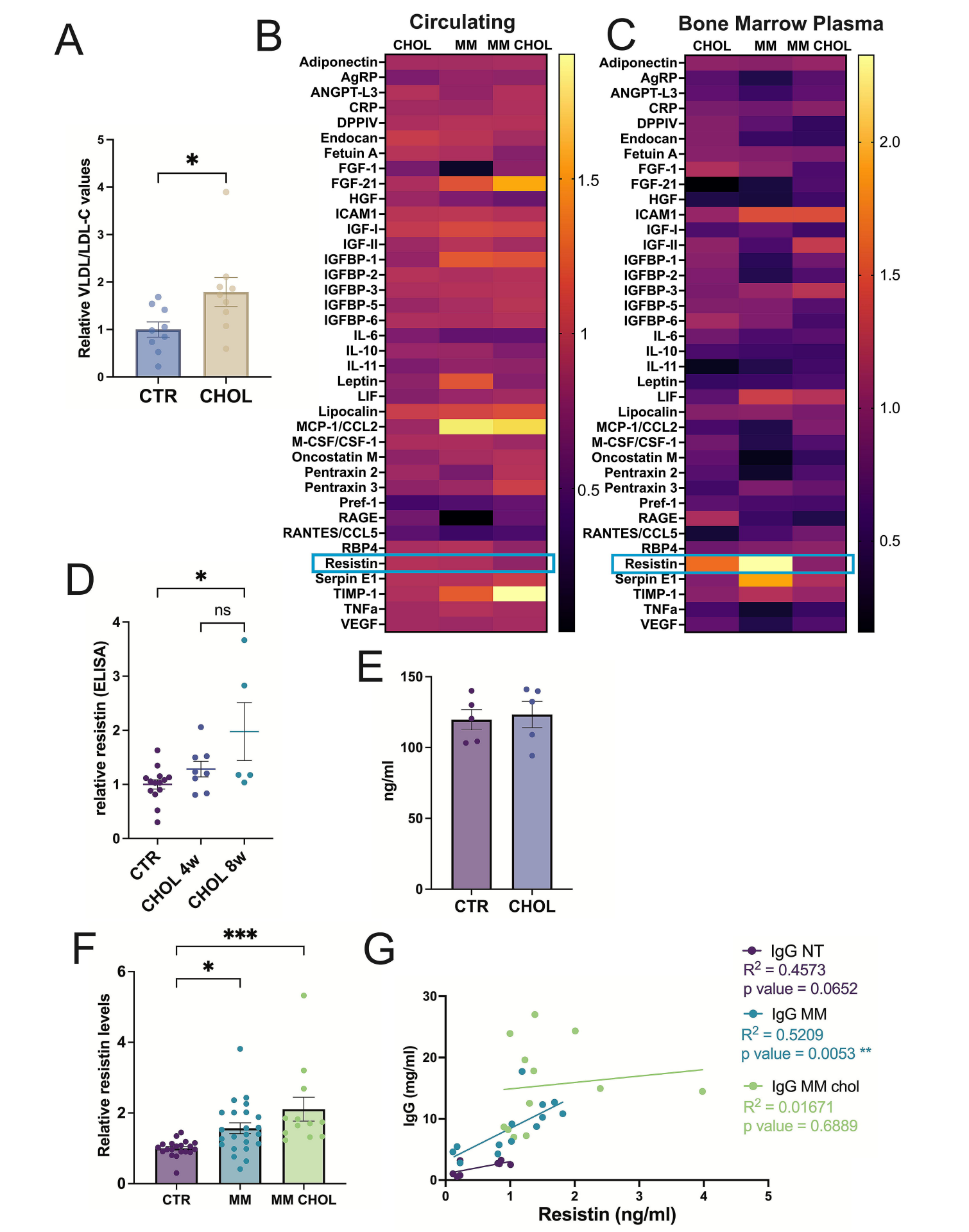
A
Relative VLDL/LDL-C values
CTR
CHOL
B
Circulating
CHOL
MM
MM CHOL
Adiponectin
AgRP
ANGPT-L3
CRP
DPPIV
Endocan
Fetuin A
FGF-1
FGF-21
HGF
ICAM1
IGF-I
IGF-II
IGFBP-1
IGFBP-2
IGFBP-3
IGFBP-5
IGFBP-6
IL-6
IL-10
IL-11
Leptin
LIF
Lipocalin
MCP-1/CCL2
M-CSF/CSF-1
Oncostatin M
Pentraxin 2
Pentraxin 3
Pref-1
RAGE
RANTES/CCL5
RBP4
Resistin
Serpin E1
TIMP-1
TNFa
VEGF
C
Bone Marrow Plasma
D
relative resistin (ELISA)
ns
CTR
CHOL 4w
CHOL 8w
E
ng/ml
F
Relative resistin levels
G
IgG (mg/ml)
Resistin (ng/ml)
IgG NT
R2 = 0.4573
p value = 0.0652
IgG MM
R2 = 0.5209
p value = 0.0053 **
IgG MM chol
R2 = 0.01671
p value = 0.6889

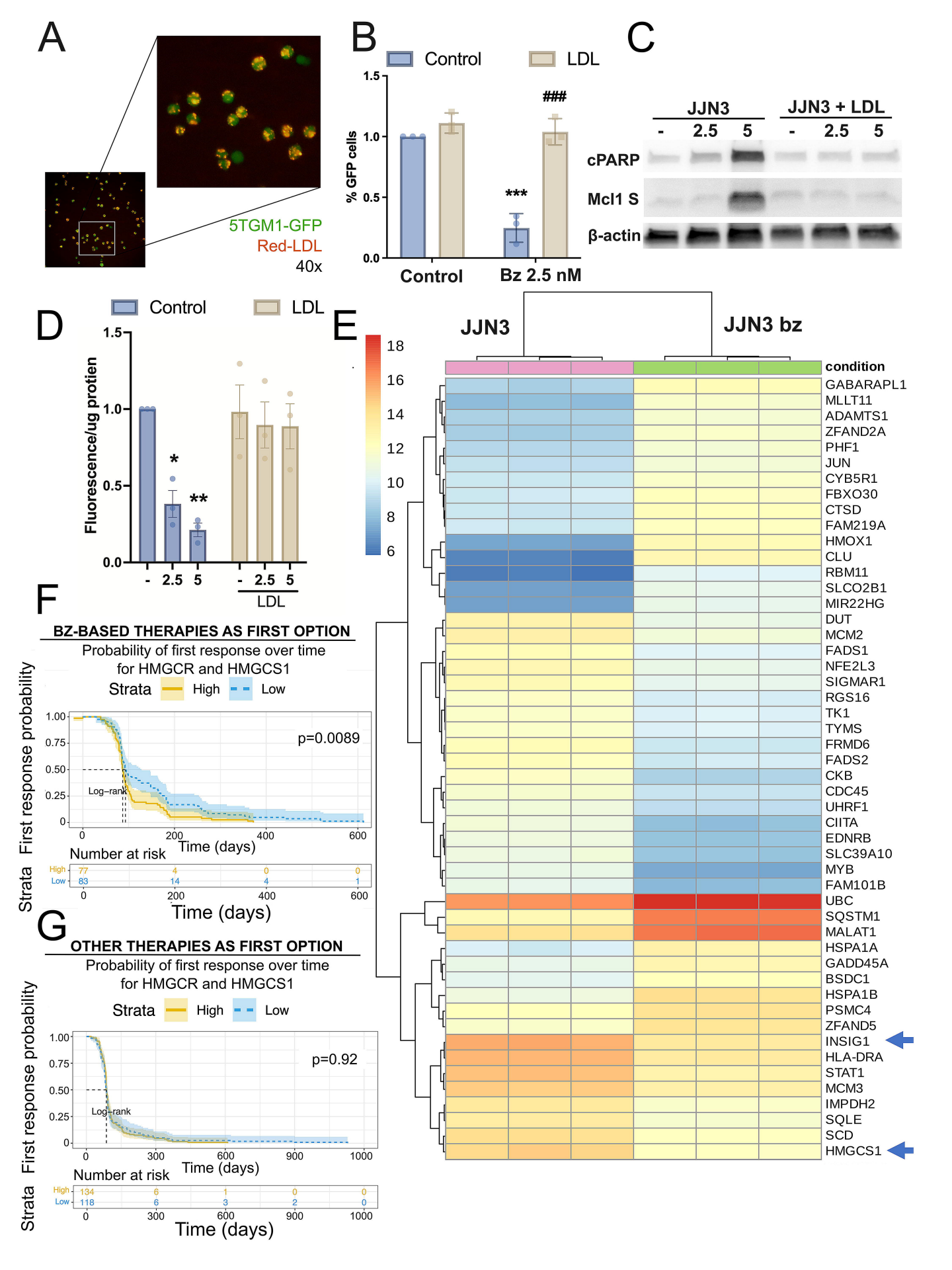
A
5TGM1-GFP
Red-LDL
40x
B
Control
LDL
% GFP cells
1.5
1.0
0.5
0.0
###
***
Control
Bz 2.5 nM
C
JJN3
JJN3 + LDL
- 2.5 5 - 2.5 5
cPARP
Mcl1 S
β-actin
D
Control
LDL
Fluorescence/ug protien
1.5
1.0
0.5
0.0
*
**
- 2.5 5 - 2.5 5
LDL
E
JJN3
JJN3 bz
18
16
14
12
10
8
6
condition
GABARAPL1
MLLT11
ADAMTS1
ZFAND2A
PHF1
JUN
CYB5R1
FBXO30
CTSD
FAM219A
HMOX1
CLU
RBM11
SLCO2B1
MIR22HG
DUT
MCM2
FADS1
NFE2L3
SIGMAR1
RGS16
TK1
TYMS
FRMD6
FADS2
CKB
CDC45
UHRF1
CIITA
EDNRB
SLC39A10
MYB
FAM101B
UBC
SQSTM1
MALAT1
HSPA1A
GADD45A
BSDC1
HSPA1B
PSMC4
ZFAND5
INSIG1
HLA-DRA
STAT1
MCM3
IMPDH2
SQLE
SCD
HMGCS1
F
BZ-BASED THERAPIES AS FIRST OPTION
Probability of first response over time
for HMGCR and HMGCS1
Strata High Low
First response probability
p=0.0089
Log−rank
Time (days)
Number at risk
High 77 4 0 0
Low 83 14 4 1
Strata
G
OTHER THERAPIES AS FIRST OPTION
Probability of first response over time
for HMGCR and HMGCS1
Strata High Low
First response probability
p=0.92
Log−rank
Time (days)
Number at risk
High 134 6 1 0 0
Low 118 6 3 2 0
Strata

SUPPLEMENTARY FIGURES

Supplementary figure 1. Cholesterol diet does not increase body weight or spleen weight but induces signs of fatty liver.

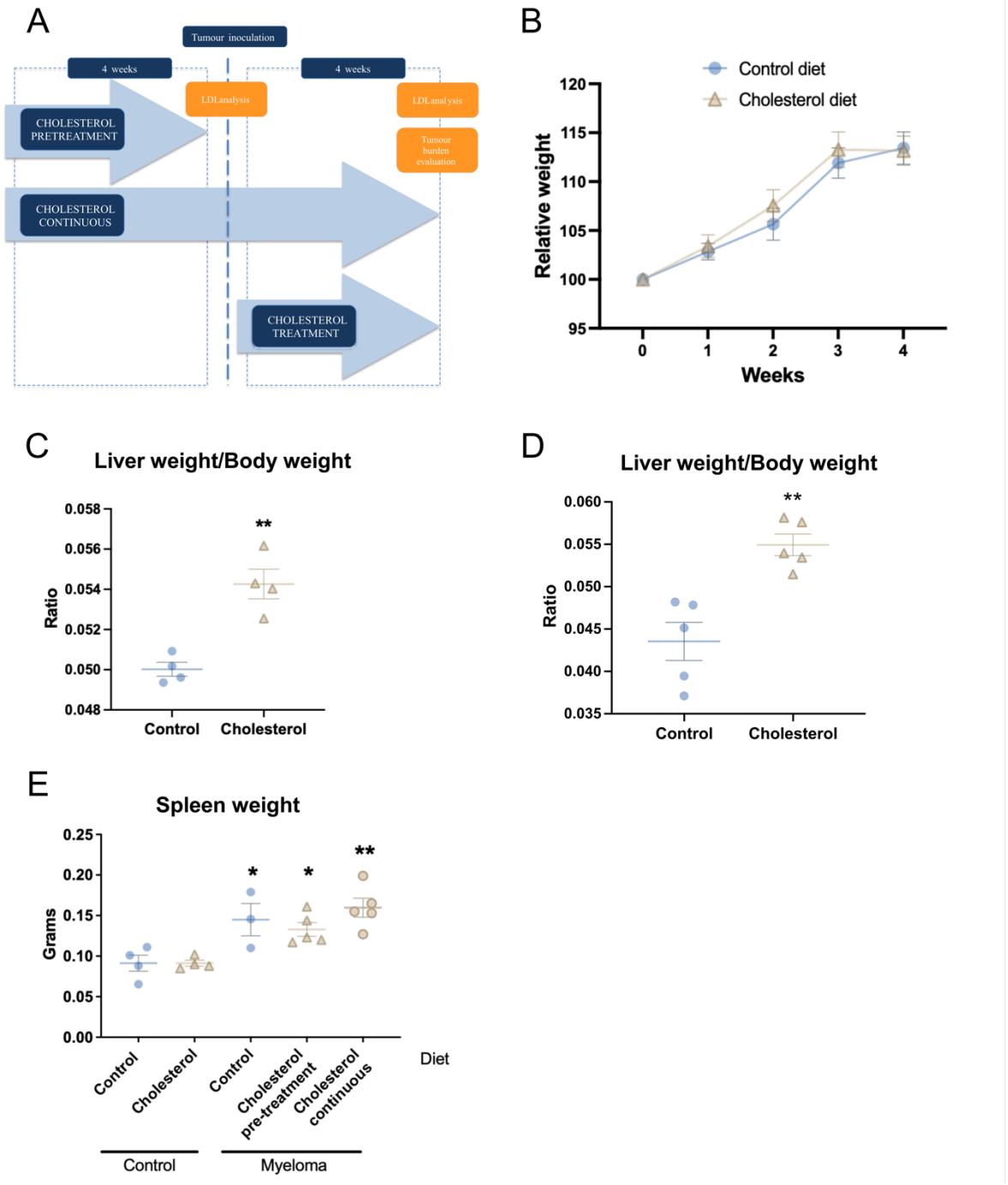

Supplementary figure 1. Cholesterol diet does not increase body weight or spleen weight but induces signs of fatty liver.

(**A**) Schematic figure showing the experimental setting for in vivo experiments. Mice were fed with either control or high cholesterol diet for 4 weeks and serum LDL was measured. Then animals were randomly distributed into either control or tumour-bearing mice (myeloma) and inoculated with 5TGM1-GFP cells. Cholesterol pre-treatment myeloma mice had cholesterol diet halted at time of inoculation whereas cholesterol continuous group were fed with cholesterol diet until sacrifice, where tumour burden was assessed. In separate experiments, cholesterol diet was introduced at time of tumour inoculation (cholesterol treatment). (**B**) C57BL/6 KaLwRij body weight after 4 weeks of high cholesterol diet. (**C**) Liver weight/body weight ratio in control and cholesterol-fed animals for 4 weeks. (**D**) Liver weight/body weight ratio in control and cholesterol-fed animals for 8 weeks. (**E**) Spleen weights where the diet was given pre-inoculation (cholesterol pre-treated) or continuously before and after tumour inoculation (cholesterol continuous). For 2 group comparison, two-tailed Student's t-test was performed. $^{**}p < 0.01$. For more than 2 groups one-way anova analysis was performed. If not otherwise indicated, $^{*}p< 0.05$, $^{**}p < 0.01$ compared to control with no-tumour. Results are presented as mean ± SEM.

Supplementary figure 2: Effect of LDL on myeloma cell viability

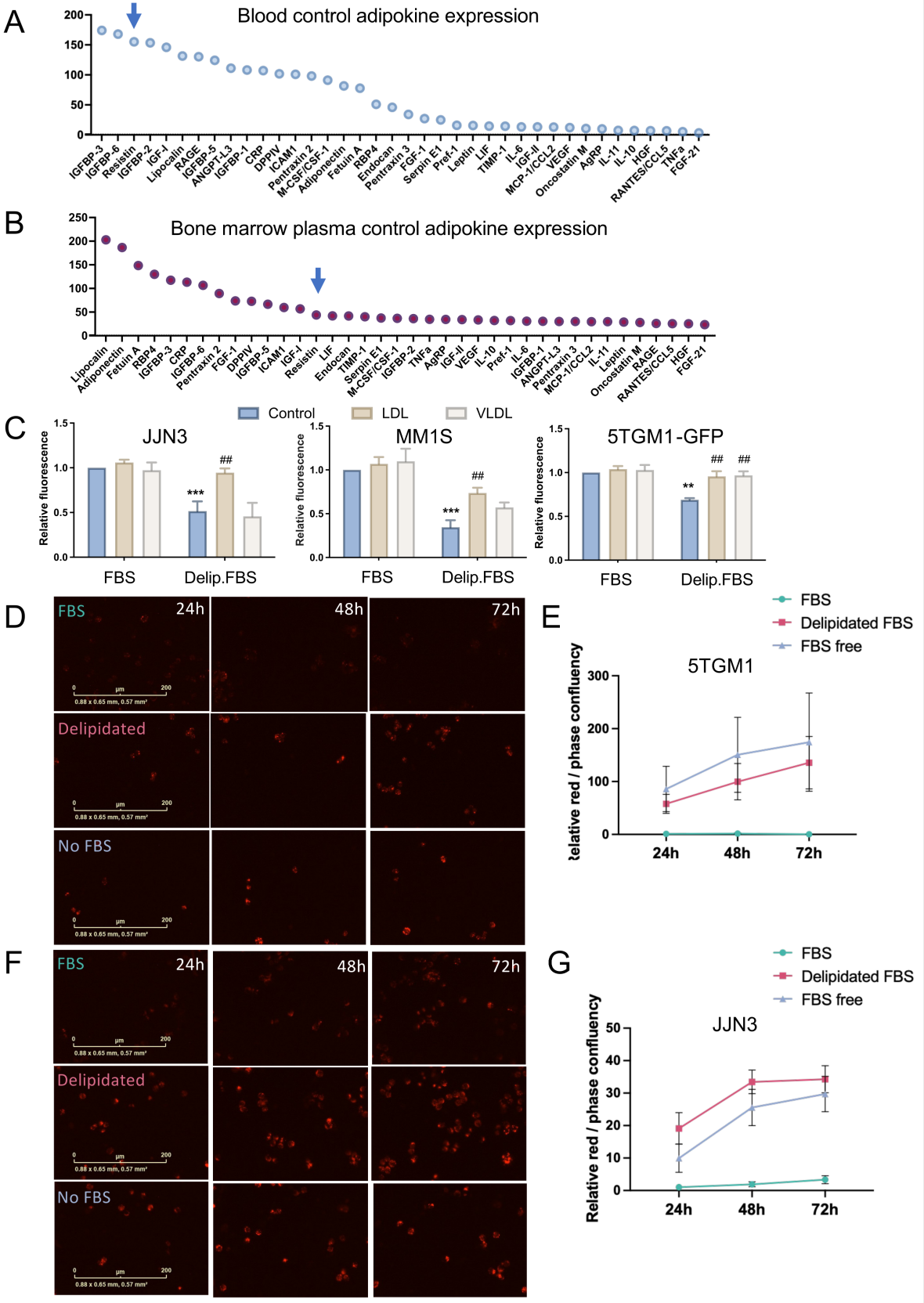

Supplementary Figure 2. Effect of LDL on myeloma cell viability

Relative expression of adipokines in blood **(A)** and bone marrow plasma **(B)** of non-tumour C57Bl/KaLWRIj mice. (**C**) JJN3, MM1s and 5TGM1-GFP cells were cultured in 10% FBS media or lipid-depleted media ± 6 µg/ml LDL or VLDL. Viability was assessed after 72 (JJN3, MM1s) or 96 hours (5TGM1) . 5TGM1-GFP (**D & E**) and JJN3 (**F & G**) were seeded using 10% FBS media, delipidated FBS media or serum free media together with Red-LDL for 24, 48 or 72 hours. Images were taken using Incucyte®Live-Cell analysis system (**D & F**). Quantification was performed using confluency of red signal over confluency of bright images (n=3) (**E & G**). For C $**p < 0.01$ and $***p < 0.001$ compared to control FBS condition. $##p < 0.01$ compared to control delipidated condition. Results are presented as mean ± SEM.

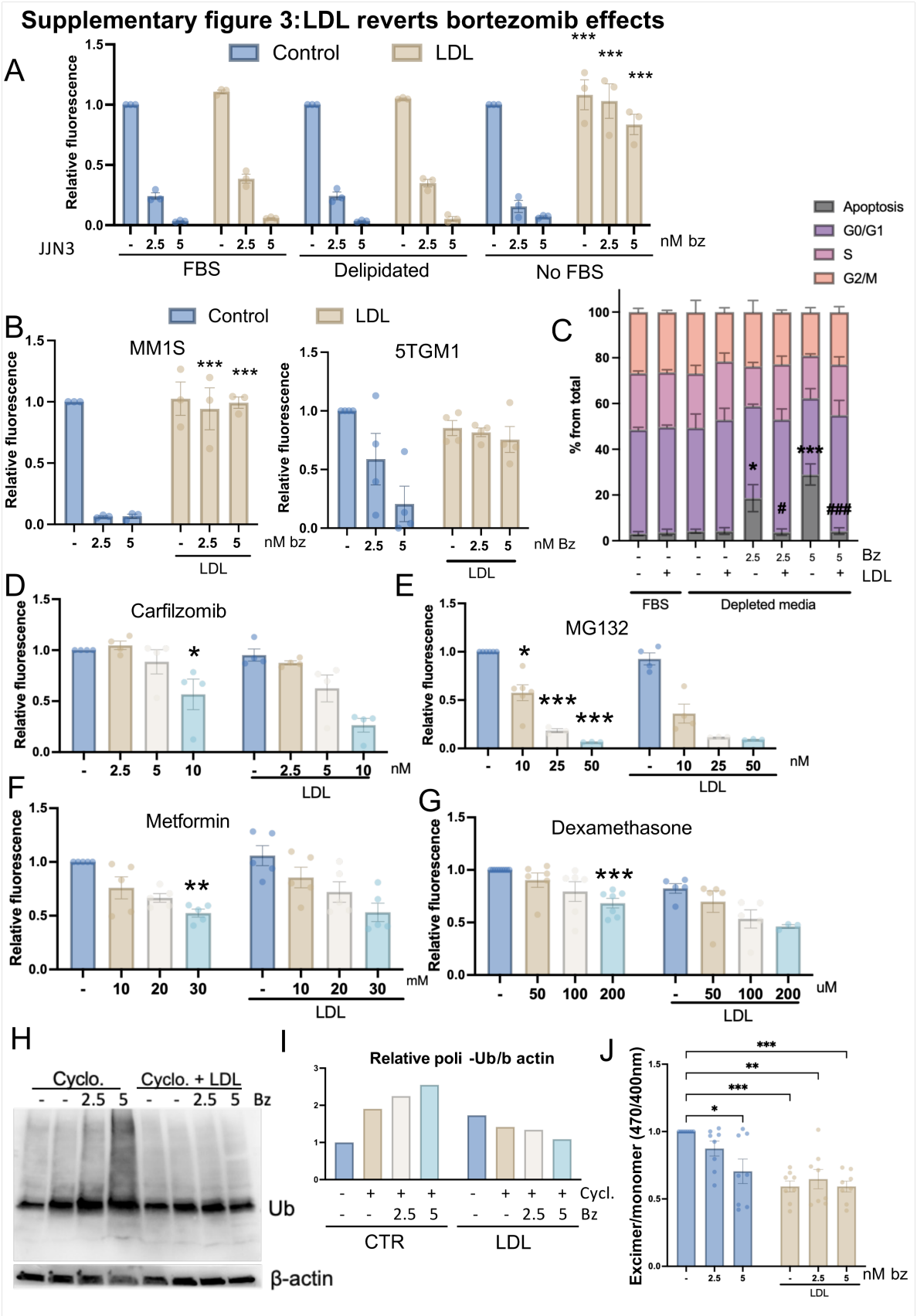
Supplementary figure 3:LDL reverts bortezomib effects
A
Control
LDL
Relative fluorescence
JJN3
FBS
Delipidated
No FBS
nM bz
Apoptosis
G0/G1
S
G2/M
B
MM1S
5TGM1
Control
LDL
nM bz
nM Bz
C
% from total
Bz
LDL
FBS
Depleted media
D
Carfilzomib
nM
E
MG132
F
Metformin
mM
G
Dexamethasone
uM
H
Cyclo.
Cyclo. + LDL
Bz
Ub
β-actin
I
Relative poli -Ub/b actin
Cycl.
CTR
J
Excimer/monomer (470/400nm)

Supplementary Figure 3. LDL reverts bortezomib effects

(**A**) JJN3 cells were cultured in 10% FBS, delipidated or no FBS media and treated with 30 µg/ml LDL for 3 hours before 24 hour bortezomib treatment (2.5 or 5nM). Viability was quantitated by alamar blue (n = 3). (**B**) MM1S and 5TGM1 cells were cultured in no FBS media and treated was (A). Viability was quantitated by alamar blue (n = 3-4). (**C**) JJN3 were cultured in serum-free conditions ± LDL for 3 hours before bortezomib treatment for 24 hours and cell cycle analysis was performed using propidium iodide. JJN3 cells were treated with carfilzomib (**D**), MG132 (**E**), Metformin (**F**) or Dexamethasone (**G**) ± LDL. Cycloheximide experiments were performed and proteasome activity assessed by expression of poli-ubiquitin. (**H**) Representative western-blot and (**I**) quantification (as relative ubiquitin signal/β-actin) shows ubiquitinated-protein accumulation (n=3). (**J**) Changes in membrane fluidity were evaluated. For A ***$p < 0.001$ compared to control non-LDL condition. For D-G & J, *$p< 0.05$, **$p < 0.01$, ***$p < 0.001$ compared to control (no bortezomib, no LDL).

Supplementary figure 4. LDL restores the gene expression signature of bortezomib treated myeloma cells.

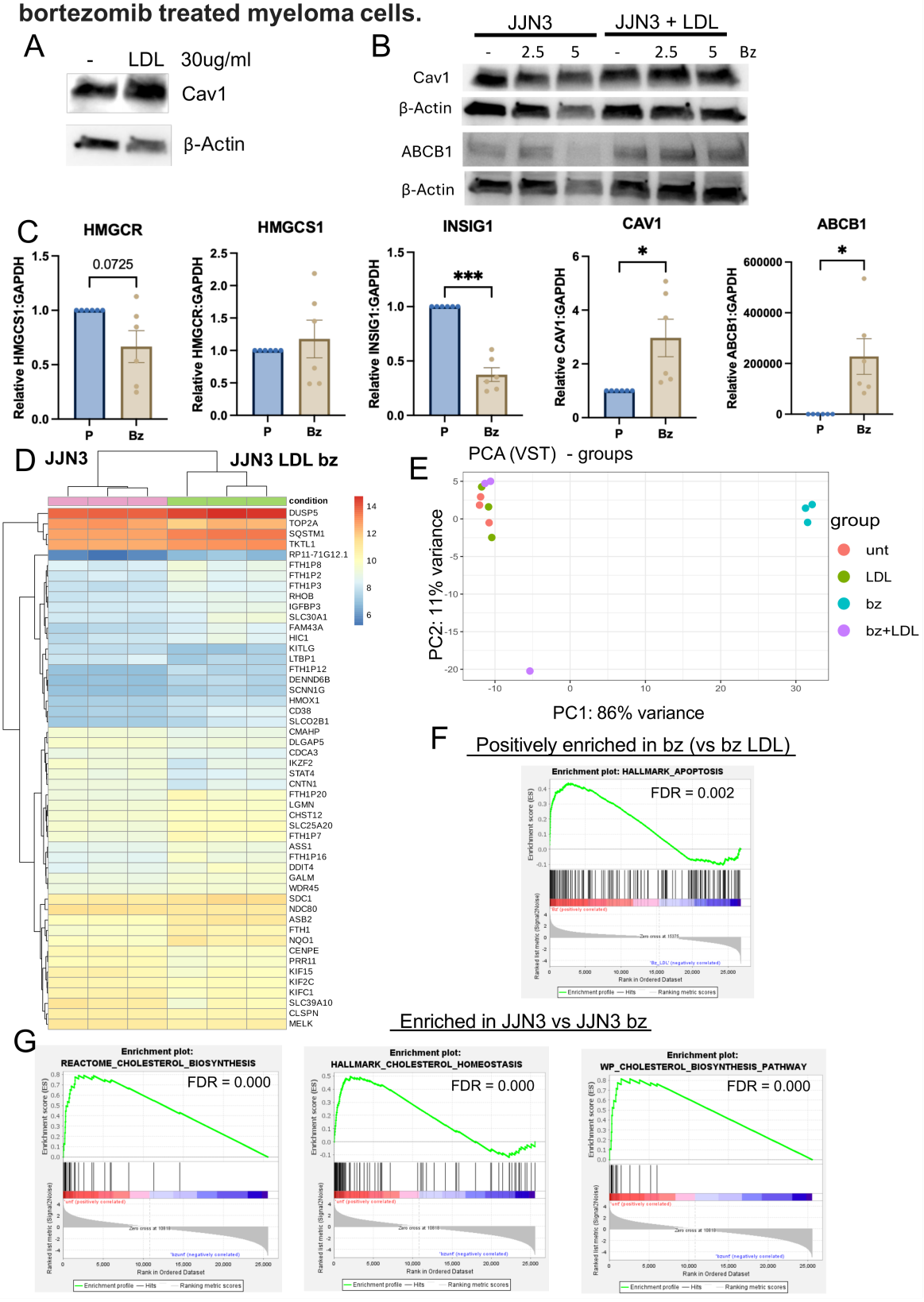

Supplementary Figure 4. LDL restores the gene expression signature of bortezomib treated myeloma cells.

(**A**) Expression of caveolin-1 on JJN3 myeloma cells after 30μg/ml LDL treatment for 24. (**B**) Expression of caveolin-1 and MDR/ABCB1 protein in JJN3 cells treated as per drug resistance experiments. (**C**) Expression of cholesterol-related genes in bortezomib resistant (Bz) and parental (P) L363 myeloma cells. (**D**) JJN3 myeloma cells were treated in the presence and absence of LDL and bortezomib and RNA-Seq performed. Heatmap showing DEG analysis of JJN3 vs. JJN3 LDL + bortezomib. (**E**) PCA plot from untreated (unt), bortezomib (bz), LDL treated (LDL) and LDL + bortezomib (bz + LDL) groups. (**F**) Bortezomib vs. bortezomib + LDL GSEA enrichment plot of HALLMARK_APOPTOSIS gene set. (**G**) Control vs. bortezomib GSEA enrichment plot of reactome cholesterol biosynthesis, hallmark cholesterol homeostasis and WP cholesterol biosynthesis pathway gene sets. For C, two-tailed Student's t-test was performed. *$p < 0.05$, ***$p < 0.001$.

Supplementary figure 5: LDL treatment affects the ferroptosis pathway

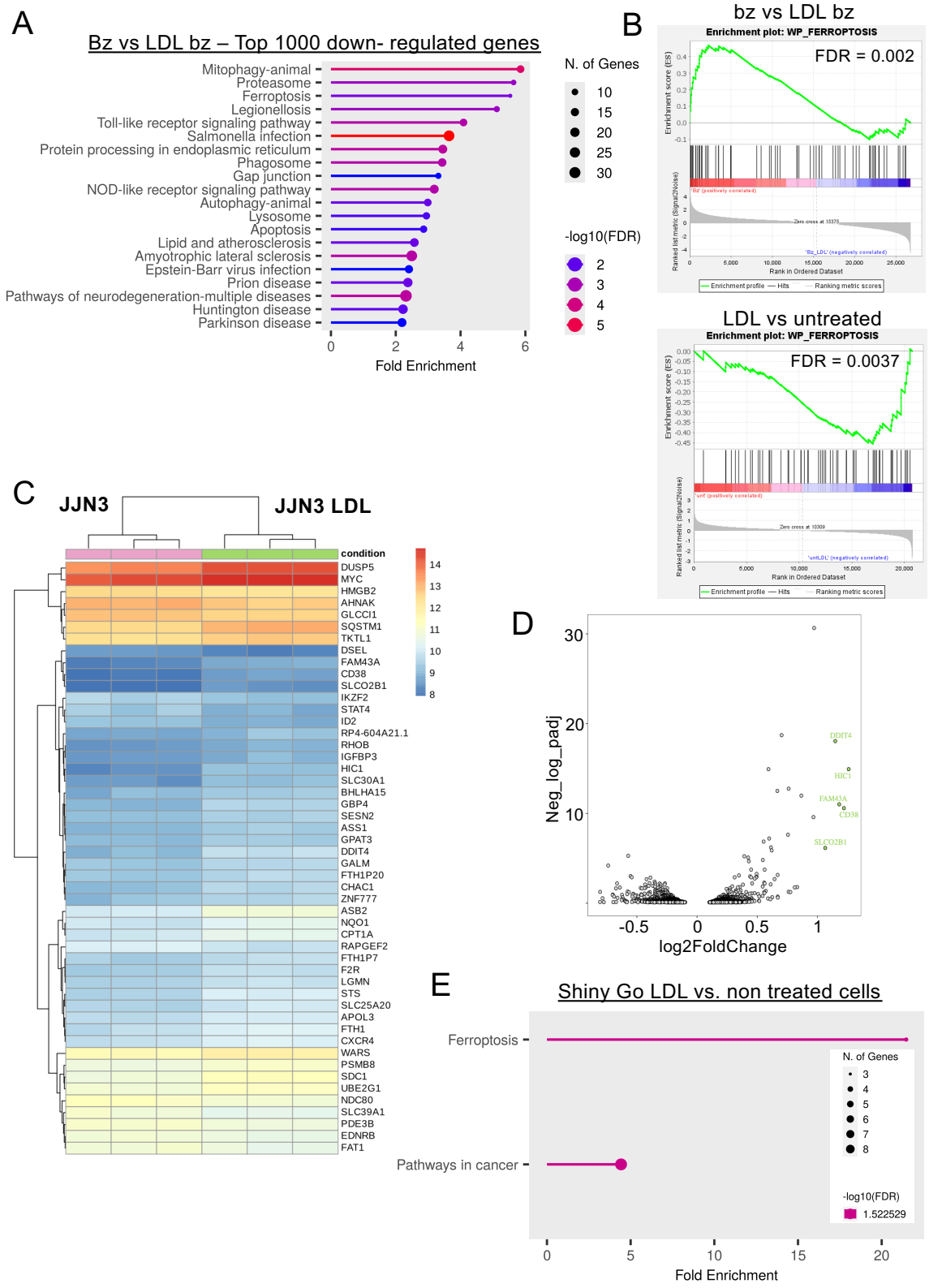

Supplementary Figure 5. LDL treatment affects ferroptosis pathway

(**A**) ShinyGO analysis of JJN3 treated with bortezomib vs LDL + bortezomib. (**B**) GSEA analysis using the WP_FERROPTOSIS gene set in bortezomib vs LDL + bortezomib and LDL vs. control . (**C**) JJN3 myeloma cells were treated in the presence and absence of LDL and bortezomib and RNA-Seq performed. Heatmap (**C**) and volcano plot (**D**) showing DEG analysis of LDL vs control. (**E**) ShinyGO analysis of differentially expressed genes in control vs. LDL.